CAPACITY OF STIFFENED STEEL SHEAR PANELS AS A STRUCTURAL CONTROL DAMPER

H.B. Ge[1], K. Kaneko[2] and T. Usami[3]

[1,3] *Professor, Department of Civil Engineering, Meijo University, Nagoya 458-8502, Japan*
[2] *Graduate Student, Department of Civil Engineering, Nagoya University, Nagoya 464-8603, Japan*
Email: gehanbin@ccmfs.meijo-u.ac.jp, kaneko@struct.civil.nagoya-u.ac.jp, usamit@ccmfs.meijo-u.ac.jp

ABSTRACT :

This paper deals with the deformation capacity of shear panel dampers (SPD), which is one type of sacrificing members to be used in damage control design of structures. The deformation capacity indexes of SPD considered are the maximum deformation and cumulative inelastic deformation, and their target values are assumed to be 12% and 280%, respectively. To investigate if the SPD is of this capacity, an extensive numerical analysis is carried out. Validity of the analytical method is verified with experimental results. It is found that the present analysis can accurately predict the inelastic cyclic behavior of high performance SPDs.

KEYWORDS: Shear dampers, Stiffened plate, Cyclic behavior, Deformation capacity

1. INTRODUCTION

A shear-type hysteretic damper (stiffened or unstiffened) is one type of various hysteretic dampers, whose effective mechanism for dissipation of energy input to a structure from an earthquake is through inelastic deformation of the metals. When a shear panel is installed into structures acting as an energy absorber, it is important to specify the range of shear deformation that the panel will sustain capacity in the event of an earthquake, namely, the limiting range of shear deformation demand. For building structures, maximum story drift of 1% is usually specified for Level II design earthquakes (Nakashima 1995). According to geometric configuration, the range of 3–5% is consequently taken as lower bound of shear deformation angle for a combined-type shear panel damper within building frames (Takahashi and Shinabe 1997). For bridge structures, limiting values of 10–12% for ultimate shear deformation angle are specified in the Guidelines (RTRI 2000) and a previous paper by Usami (2007).

Extensive experimental and analytical researches have been conducted on individual shear panel dampers and building structures incorporated with them (Nakashima et al. 1994; Tanaka and Sasaki 2000; Nakashima 1995; Takahashi and Shinabe 1997; Tanaka et al. 1999). However, the researches on bridge structures remain infancy (RTRI 2000; McDaniel et al. 2003; Chen et al. 2005; Chen et al. 2007). Recently, an experimental study on developing high-performance stiffened shear panel dampers for possible use in bridge structures was carried out by the authors (koike et al. 2008). It has been confirmed that the stiffened SPDs have high deformation capacity as large as 12% in strain and 280% in cumulative inelastic strain and high durability for low cycle fatigue by installing the stiffeners adequately. In this paper, analytical results of stiffened steel shear panel dampers under cyclic shear loading are presented, and compared with the experiment (Koike et al., 2008).

2. ANALYTICAL METHOD

2.1 Main Parameters

The schematic of SPD is shown in Fig.1. The web slenderness parameter and the rigidity of stiffeners are two important parameters in considering shear deformation in web, because shear buckling is undesirable to dissipate enough energy or in other words hysteretic loops should be stable. The web slenderness parameter R_w is defined as

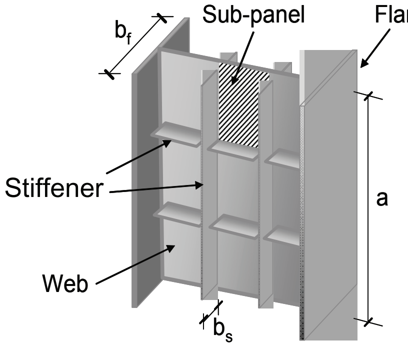

Figure 1 SPD

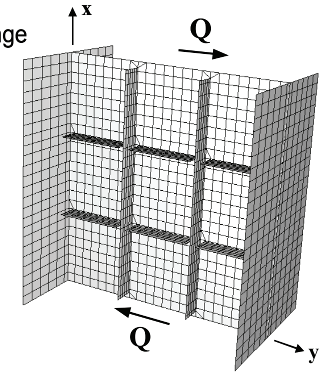

Figure 2 FEM model

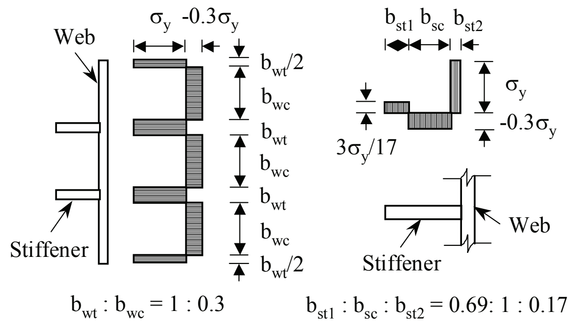

(a)web (b)stiffener

Fig.3 Distribution of residual stresses

$$R_w = \frac{b_w}{t_w}\sqrt{\frac{12(1-\nu^2)\tau_y}{k_s \pi^2 E}} \tag{2.1}$$

where b_w and t_w=width and thickness of web respectively, τ_y=shear yield stress of web material ($=\sigma_y/\sqrt{3}$), E=Young's modulus of elasticity, ν=Poisson's ratio, and k_s=elastic buckling coefficient of a simply-supported plate under shear, given by

$$k_s = \begin{cases} (n_L+1)^2\left(5.35+4/\alpha_s^{\,2}\right) & \alpha_s \geq 1 \\ (n_L+1)^2\left(5.35/\alpha_s^{\,2}+4\right) & \alpha_s \leq 1 \end{cases} \tag{2.2}$$

where n_L=number of longitudinal stiffeners, and α_s=aspect ratio of subpanel. As described in Eq.(2.1), when b_w(= height "a" in this study) gets large, there are two way to keep R_w constant. One way is to use a thicker plate, and another way is to add stiffeners. In the former way, it is undesirable for the yield load of SPD to get larger because SPD should yield earlier than main structure to perform hysteretic damping. Thus, the latter way is effective and considered in this study.

The rigidity of stiffeners γ_s is defined as

$$\gamma_s = \frac{E \cdot I_s}{b_w \cdot D_w} \tag{2.3}$$

where I_s=moment of inertia of stiffener, taken at the interaction surface of stiffener and web, and D_w=flexural rigidities per unit width of web. In this study, rigidity of stiffeners is designed with 3 times of optimum rigidity of stiffeners γ_s*, defined as

$$\gamma_s^{\,*} = \left(\frac{23.1}{n_L^{\,2.5}} - \frac{1.35}{n_L^{\,0.5}}\right) \cdot \frac{\left(1+\alpha^{3/n_L-0.3}\right)^{2n_L-1}}{1+\alpha^{5.3-0.6n_L-3/n_L}} \tag{2.4}$$

Analytical models designed in this study are shown in Table 1. The numbers after letters "SPD" in the model names are the web slenderness parameter and the number of stiffeners, respectively. Stiffener locates both side of web except for SPD-0.20-2A.

To make sure that hysteretic damper have enough performance in earthquake, the yield of SPD must be prior to that of main structure, as referred above. In this study, low- yielding-point steel LY225, whose yield point is controlled in a limited range, is used for the web and SM490Y for stiffeners and flange. Table 2 shows the material properties.

2.2 Analytical Model

The analysis is performed with general-purpose finite element program ABAQUS (2003). The web, stiffener and flange are modeled by 3-dimensional reduced-integration shell elements as shown in Fig.2. The modified two surface model is employed as constitutive law in order to trace the material cyclic behavior accurately (Shen et al., 1995). Additionally, initial imperfection, residual stress and initial deflection, are also considered. The distribution of the residual stress in the web and the stiffeners is idealized in a rectangular pattern, as shown in Fig.3. On the other hand, initial out-of-plane deflection in web is assumed as

$$\delta_w = -\frac{a}{1000}\sin\left(\frac{\pi x}{a}\right)\sin\left(\frac{\pi y}{b_w}\right) + \frac{b_w}{150(n_L+1)}\sin\left(\frac{(n_L+1)\pi x}{a}\right)\sin\left(\frac{(n_L+1)\pi y}{b_w}\right) \tag{2.5}$$

Considering that both ends of the panel are welded on considerably rigid plate in practice, the degree of freedom of the model at the planes x=0 and x=a (see Fig.2) are assumed fixed except for the displacement in the x and y directions. Cyclic displacement loading pattern is employed as the same as in the experiment (Koike et al. 2008). It is executed with an increment of 2% average shear strain alternating with positive and negative, as defined in Eq.(2.6), until 12% and after reaching 12% constant amplitude loading is performed until cumulative plastic deformation reaches 280%. In this study, pure shear is considered without considering the effect of vertical load.

During the analysis, average shear stress, τ_n, and average shear strain, γ, are defined in Eq.(2.6).

$$\tau_n = \frac{Q}{b_w \cdot t_w} \quad , \quad \gamma = \frac{\delta}{a} \tag{2.6}$$

where Q=summation of horizontal reaction forces at the plane x=0.

Table 1 Structural parameters and dimensions of SPD

Model	R_w (Design value)	Web							Stiffener					Flange	
		a	b_w	t_w	α	α_s	b_w/t_w	R_w	n_L	n_T	b_s	t_s	γ_s/γ_s*	b_f	t_f
		mm	mm	mm							mm	mm		mm	mm
①SPD-0.25-0	0.25	400	400	14.00	1.0	1.0	29	0.235	—	—	—	—	—	300	19
②SPD-0.125-1	0.125	400	400	14.00	1.0	1.0	29	0.126	1	1	82	14	3.00	300	19
③SPD-0.20-1	0.20	500	500	11.00	1.0	1.0	45	0.201	1	1	77	11	3.02	350	22
④SPD-0.20-2	0.20	610	610	9.00	1.0	1.0	68	0.204	2	2	59	9	3.01	400	25
⑤SPD-0.20-2A	0.20	610	610	9.00	1.0	1.0	68	0.204	2	2	80	9	3.00	400	25
⑥SPD-0.20-1/2	0.20	407	610	9.00	0.67	1.0	68	0.204	1	2	59	9	3.01	400	25
⑦SPD-0.30-1	0.30	610	610	9.00	1.0	1.0	68	0.306	1	1	72	9	3.00	400	25

Table 2 Material properties

Steel	E (GPa)	σ_y (MPa)	ε_y	ν	E_{st} (MPa)	ε_{st}	σ_u (MPa)	ε_u (%)
SM490Y(9mm)	206	413	0.00200	0.296	6.56	0.0130	547	25.9
SM490Y(11mm)	214	496	0.00232	0.303	3.78	0.0210	599	23.5
SM490Y(14mm)	205	482	0.00235	0.293	5.47	0.0112	594	25.1
SM490Y(19mm)	213	437	0.00205	0.286	5.13	0.0182	554	29.0
SM490Y(22mm)	209	397	0.00190	0.286	5.58	0.0130	541	26.8
SM490Y(25mm)	205	435	0.00213	0.289	5.66	0.0144	565	27.4
LY225(9mm)	200	242	0.00121	0.294	2.48	0.0246	320	57.4
LY225(16mm)	212	237	0.00112	0.300	1.83	0.0228	328	63.6

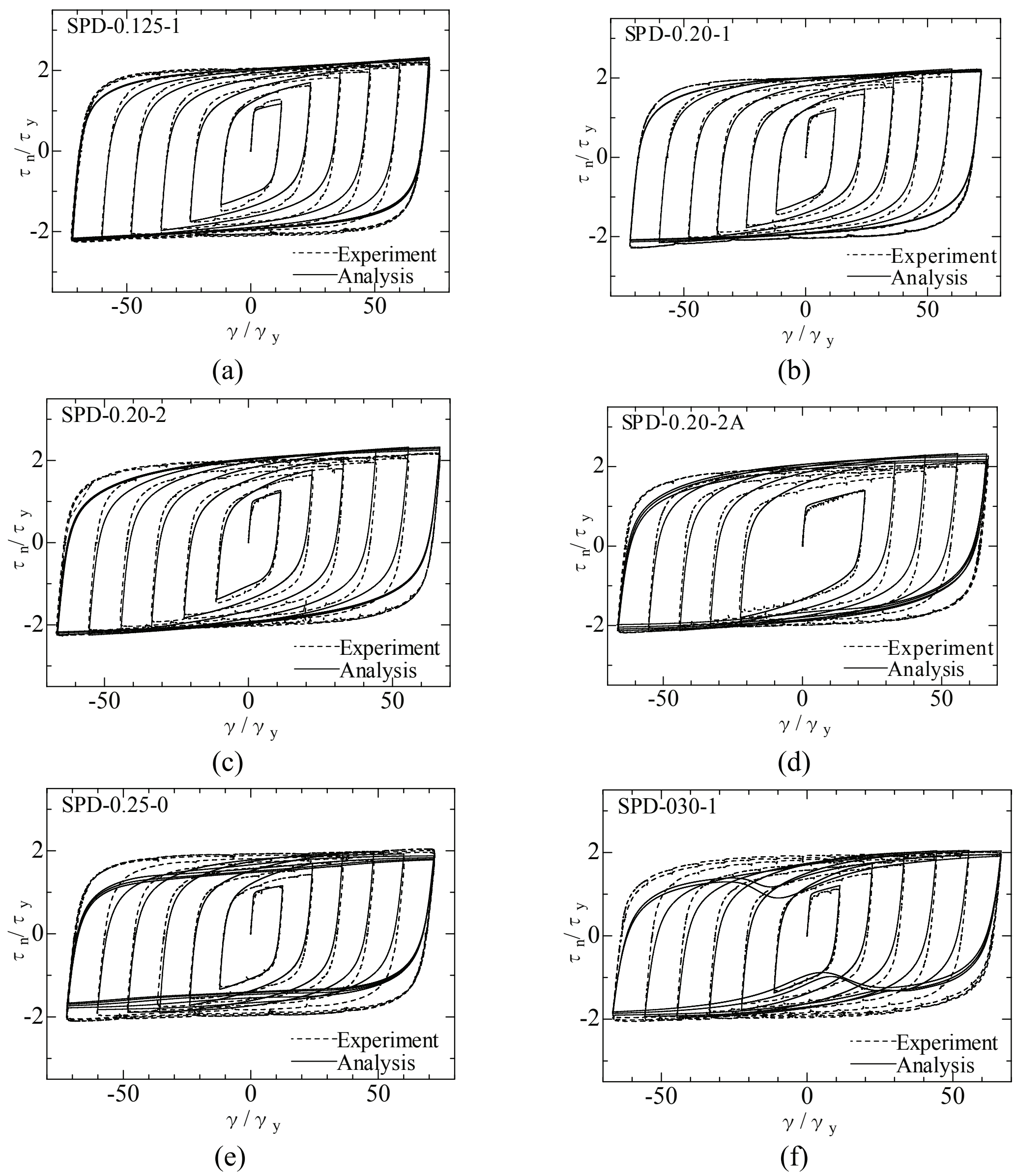

Figure 4 Hysteretic shear stress-shear strain curves

3. RESULTS AND COMMENTS

Figure 4 shows typical hysteretic curves of the normalized shear stress versus shear strain of several analytical models compared with corresponding experimental curves. As can be seen from Fig.4, hysteretic curves obtained from the analysis agree generally well with those from the experiment, although the gradient in hardening region is somewhat different between experiment and analysis in all the models.

In the analysis, the strength deterioration occurs at an average shear strain of -6% or 8% in the case of SPD-0.25-0 (Fig.4(e)) and the pinching occurs after reaching 12% in the case of SPD-0.30-1(Fig.4(f)). On the other hand, in the cases of SPD-0.125-1 and R_w =0.2 series such as SPD-0.20-1 and SPD-0.2-2 the analytical hysteretic curves agree with the experimental results with a good accuracy, because shear strength deterioration was not observed in the analysis before the target capacity (12% of the maximum strain and 280% of the cumulative strains). It should be noted that in final several cycles of the analysis the shear strength deterioration

(a)overall view after test (b)detail on left side (c)detail on right side

Figure 5 Crack propagation in tested specimen SPD-0.20-2

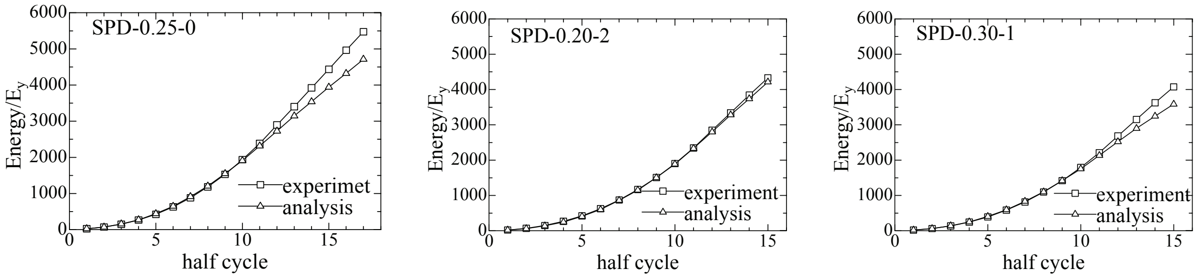

Fig.6 Cumulative dissipated energy

occurred due to local buckling.

In the experiment both the local buckling in sub-panels and crack propagation around edge of stiffeners initiated by extremely low-cycle fatigue were observed although the strength deterioration is hardly observed in the specimens with smaller values of the width-thickness ratio, as shown in Fig.4. Figure 5 shows cracks around edge of stiffeners in the case of SPD-0.20-2 after test. The crack firstly took place on boxing of stiffener, which ties fillet weld on both sides of the stiffener, and propagated in the thickness direction. In the present analytical model, however, the crack initiation and propagation are not considered. But the shear strength keeps increasing for a while after crack initiation which happened before 280% of the cumulative inelastic deformation.

Refer to the required capacity describing above, all the models used in this study satisfied in both experiment and analysis except for analytical model of SPD-0.30-1, whose hysteretic loop seems unstable as shown in Fig.4. It is also found that the web slenderness parameter R_w is a controlling parameter in determining the capacity. And in order to have designed strength against buckling, the stiffeners need to work in good condition until the end of the loading. In this study stiffeners are designed as 3 times of optimum rigidity of stiffeners γ_s* as referred above, and such a design consideration is appropriate since the buckling occurred at nodes of stiffeners as shown in Fig.5.

Comparisons of SPD-0.2-2 with stiffeners at one side and SPD-0.20-2A with stiffeners at both sides show that there is no obvious difference either in the hysteretic loops or in deformation capacities, although a little difference was observed in the experiments. This is because that in the case of SPD-0.2-2 crack initiated on only one side of the web and got delayed to go through in the thickness direction, compared with SPD-0.2-2A.

When SPD-0.20-1 with the same value of R_w but only one stiffener is compared with SPD-0.20-2, the cumulative inelastic deformation in the case of SPD-0.20-1 is almost the same to that of SPD-0.20-2

The cumulative inelastic deformation of several models are shown in Fig.6. In Fig.6, The vertical axis represents the cumulative dissipated energy which is normalized with E_y($=Q_y\Delta_y/2$) and horizontal axis represents half cycle which counts γ=+2%, -2%, +4%⋯ as 1, 2, 3⋯ in the loading pattern. The prediction error at the final stage (i.e., the last half cycle) between the experiment and analysis is larger than 10% in the cases of SPD-0.25-0 and SPD-0.30-1, where the buckling caused considerable strength deterioration in analysis. On the other hand, in the analytical models with R_w below 0.20, the prediction error is less than 5%.

Therefore, it can be concluded that the models with R_w below 0.20 can be considered to have high performance satisfied with the capacity limits.

4. CONCLUSIONS

This paper presented results of a numerical analysis on developing high-performance stiffened steel shear panel dampers. It has been shown that the cyclic behavior and capacity of the SPDs with R_w below 0.20 can be predicted using the present analytical models with good accuracy.

This study is the first step for developing high-performance SPD with required capacity. To investigate an appropriate capacity required for SPD, dynamic analysis of structures installed with SPD has to be performed and response of SPD induced by the earthquake has to be investigated with varying parameters.

ACKNOWLEGEMENT: The study was supported in part by grants from the Advanced Research Center for Seismic Experiments and Computations, Meijo University.

REFERENCES

ABAQUS, Inc., ABAQUS/Analysis user's manual-version 6.5, Pawtucket, R.I., 2003

Chen, Z.Y., Ge, H.B., and Usami, T. (2006). Hysteretic model of stiffened shear panel dampers. *J. Struct. Eng., ASCE*:**132(3)**, 478–483.

Chen, Z.Y., Ge, H.B. and Usami T. (2007). Study on seismic performance upgrading for steel bridge structures by Introducing energy-dissipation members, *J. Struct. Eng., JSCE*:**Vol.53A**, 540-549.

Koike Y., Yanaka T., Usami T., Ge H. B., Oshita S., Sagou D., Uno Y. (2008). An experimental study on developing high-performance stiffened shear panel dampers. *J. Struct. Eng., JSCE* :**Vol.54A**, 372-381.

McDaniel, C. C., Uang, C. M., and Seible, F. (2003). Cyclic testing of built-up steel shear links for the new bay bridge. *J. Struct. Eng., ASCE*:**129(6)**, 801–809.

Nakashima, M. (1995). Strain-hardening behavior of shear panels made of low-yield steel. I: Test. *J. Struct. Eng., ASCE*:**121(12)**, 1742–1749.

Nakashima, M., Iwai, S., Iwata, M., Takeuchi, T., Konomi, S., Akazawa, T., and Saburi, K. (1994). Energy dissipation behavior of shear panels made of low yield steel. *Earthq. Eng. Struct. Dyn.*:**23(12)**, 1299–1313.

RTRI. (2000). Guidelines for design of railway viaduct with dampers and braces, Railway Technical Research Institute, Tokyo, Japan (in Japanese).

Shen, C., Mamaghani, I. H. P., Mizuno, E., and Usami, T. (1995). Cyclic behavior of structure steels. Ⅱ: theory, *J. Engng. Mech., ASCE*:**121(11)**, 1165-1172

Takahashi, Y., and Shinabe, Y. (1997). Experimental study on restoring force characteristics of shear yielding thin steel plate elements. *J. Struct. Constr. Eng., AIJ* :**494**, 107–114 (in Japanese).

Tanaka, K., and Sasaki, Y. (2000). Hysteretic performance of shear panel dampers of ultra low-yield-strength steel for seismic response control of buildings. 12WCEE (CD-Rom), Aucklan, NZ.

Tanaka, K., Sasaki, Y., and Yoneyama, S. (1999). An experimental study on hysteretic performance of shear panel dampers using different strength type of steel under static loading. *J. Struct. Constr. Eng., AIJ*:**520**, 117–124.

Usami T. (2007). Developing high-performance damage control seismic dampers, *Proc. 10th Symp. On Ductility design Method for Bridges*, 11-22.